

## Electronic Supplementary Information

### Synthesis of highly permeable Fe<sub>2</sub>O<sub>3</sub>/ZnO hollow spheres for printable photocatalysis

Yiming Li,<sup>a</sup> Kai Wang,<sup>b</sup> Jun Wu,<sup>a</sup> Li Gu,<sup>\*b</sup> Zhufeng Lu,<sup>a</sup> Xinjun Wang<sup>c</sup> and Xuebo Cao<sup>\*a</sup>

<sup>a</sup> *School of Biology and Chemical Engineering, Jiaxing University, Jiaxing, Zhejiang 314001, China.*

*E-mail: xbcao@mail.zjxu.edu.cn.*

<sup>b</sup> *School of Materials and Textile Engineering, Jiaxing University, Jiaxing, Zhejiang, 314001, China.*

*E-mail: guli@mail.zjxu.edu.cn.*

<sup>c</sup> *School of Chemistry and Chemical Engineering, Henan Normal University, Xinxiang 453007, China*

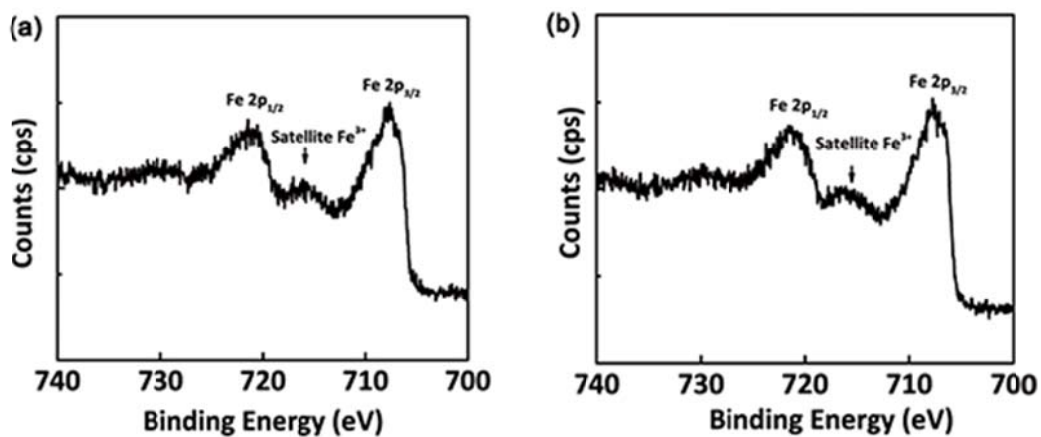


**Fig. S1** High-resolution XPS Fe 2p spectra for the as-prepared Fe<sub>2</sub>O<sub>3</sub>/ZnO hollow spheres (a) and commercial  $\alpha$ -Fe<sub>2</sub>O<sub>3</sub> nanoparticles (b). As seen, the two binding energy spectra are basically identical. Two distinct peaks at binding energies of 720.4 eV and 707.8 eV are assigned to Fe 2p<sub>1/2</sub> and Fe 2p<sub>3/2</sub>, respectively. The shake-up satellite at 716.1 eV is characteristic of Fe<sup>3+</sup> in Fe<sub>2</sub>O<sub>3</sub>.

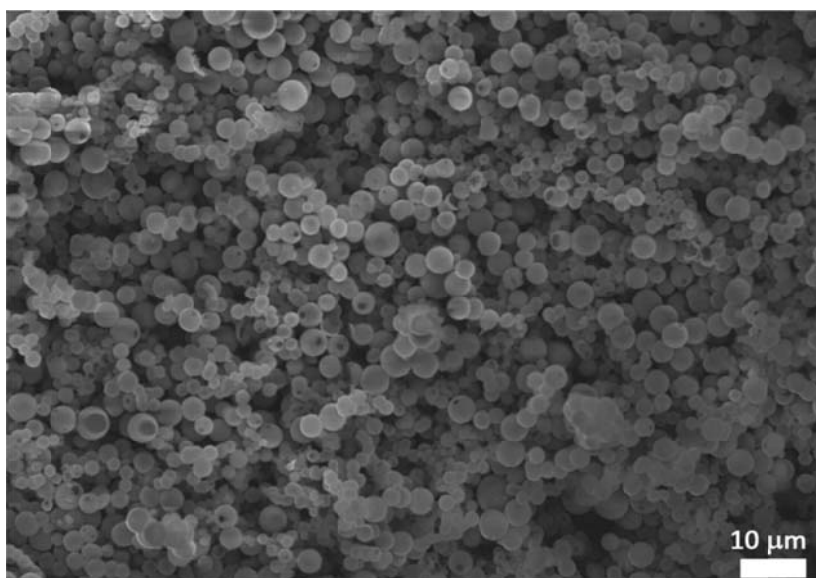


**Fig. S2** A panoramic SEM image of the mixed-phase  $\text{Fe}_2\text{O}_3/\text{ZnO}$  hollow spheres

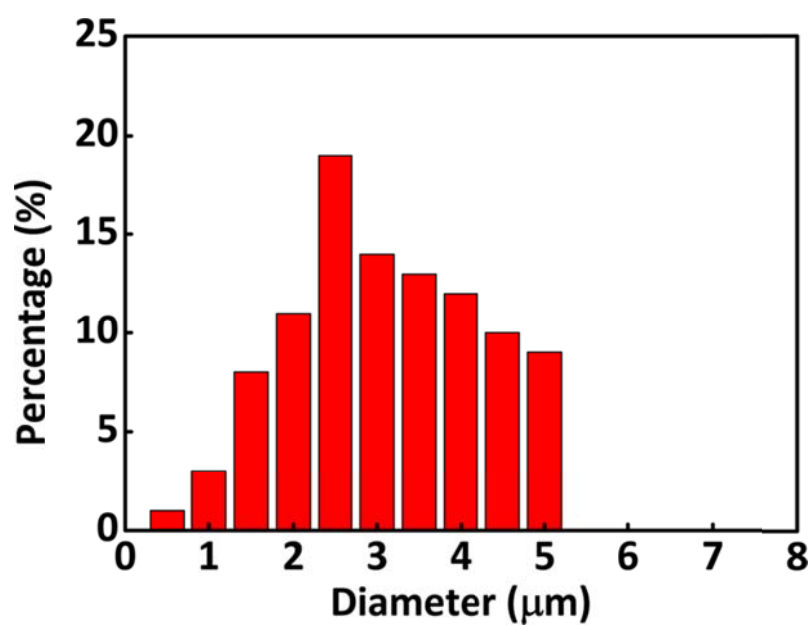


**Fig. S3** Diameter distribution for the mixed-phase  $\text{Fe}_2\text{O}_3/\text{ZnO}$  hollow spheres

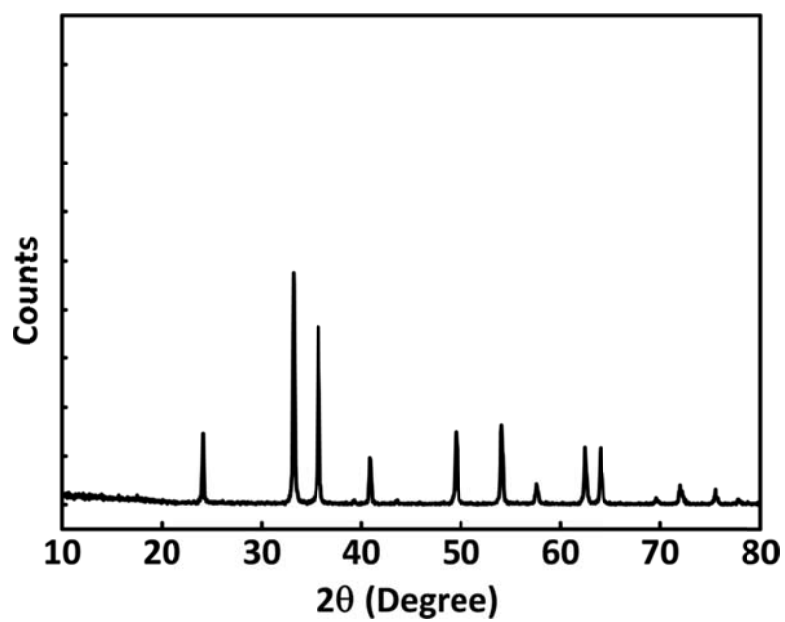


**Fig. S4** XRD pattern for the hollow spheres after etching the component of ZnO with 1 M aqueous ammonia. The result demonstrates that ZnO has been removed completely and the product is composed of pure Fe<sub>2</sub>O<sub>3</sub>.

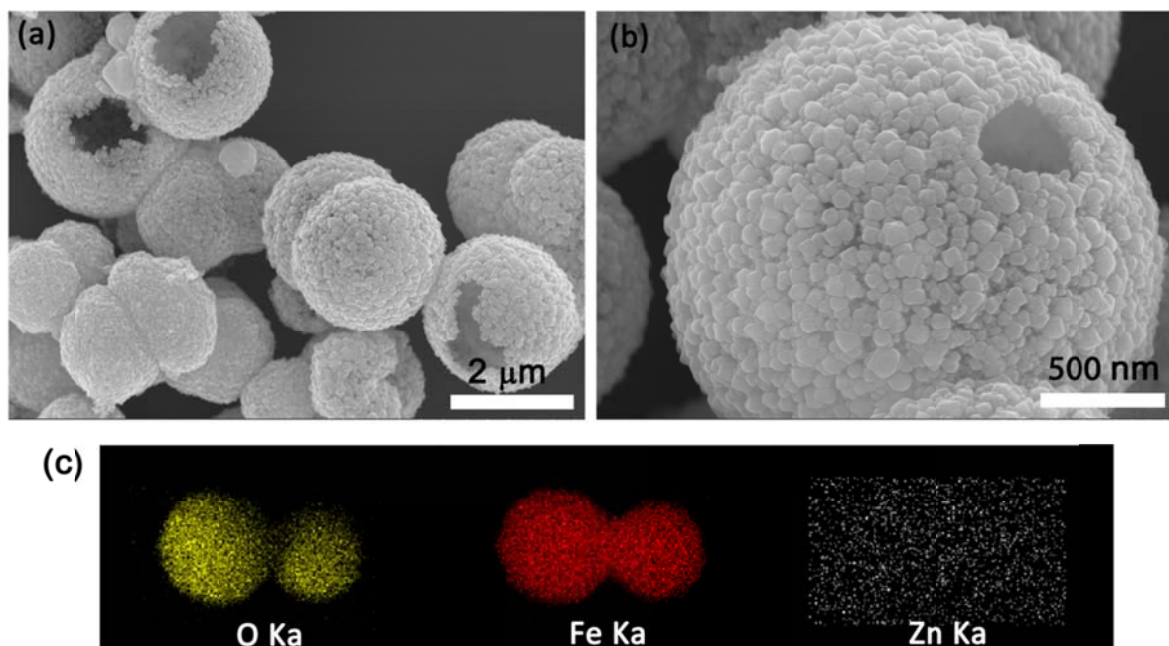


**Fig. S5** (a, b) SEM images of hollow spheres after etching the component of ZnO. (c) Corresponding elemental mapping, where the signal for Zn is disappeared. Although ZnO crystallites have been etched, the hollow spheres maintain their structures well. Meanwhile, it is clearly seen that the shell of the hollow sphere is more mesoporous owing to the removal of ZnO.

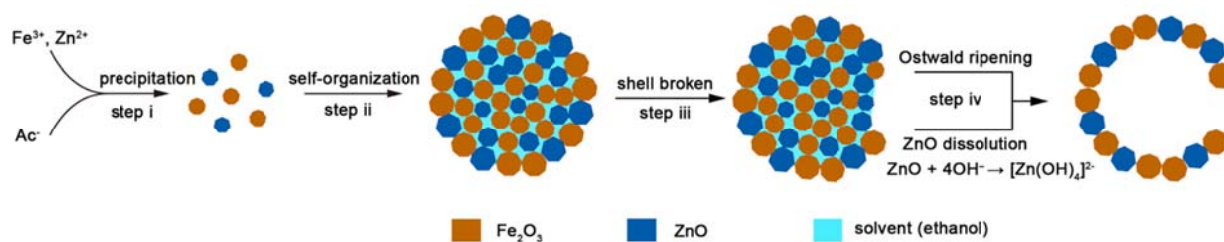


**Fig. S6** Proposed growth mechanism of the  $\text{Fe}_2\text{O}_3/\text{ZnO}$  hollow spheres with the distinct surface hole. First, the encounter of  $\text{Fe}^{3+}$  and  $\text{Zn}^{2+}$  ions to the weakly alkaline NaAc leads to the formation of ZnO and  $\text{Fe}_2\text{O}_3$  crystallites. Second, due to the demands on the reduction of the expose face and the surface free energy, ZnO and  $\text{Fe}_2\text{O}_3$  nanocrystallites are aggregated into the mixed-phase microspheres with the dense shell. At the same time, the inside of the microspheres are filled by the solvent of ethanol. Next, with the increase of the temperature of the reaction system, ethanol inside the microsphere was expanded and burst the microsphere, thus leading to the innovative surface hole. Finally, under the combination action of Ostwald ripening and amphoteric phenomenon of ZnO, smaller nanocrystallites are merged into the large ones and parts of ZnO nanocrystallites were dissolved, thus leading to the development of  $\text{Fe}_2\text{O}_3/\text{ZnO}$  hollow spheres with a relatively low ZnO percentage.

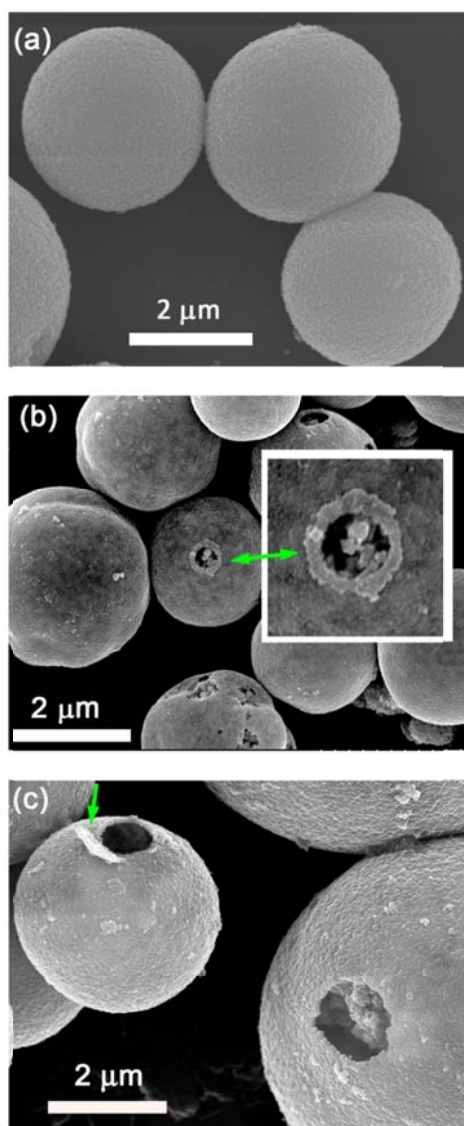


**Fig. S7.** SEM and TEM images for the intermediates observed in the growth process of the  $\text{Fe}_2\text{O}_3/\text{ZnO}$  hollow spheres. (a) Initial intermediate ( $t=1$  hour). It can be seen that the intermediate is composed of microspheres with dense shell. However, TEM image and the broken microsphere (shown in the inset) indicate that the microspheres have a porous interior. (b) Intermediates at  $t = 6$  hours. It can be seen that the surface holes have been formed. Through the hole one can see that the microspheres are filled by nanocrystallites. (c) Intermediate at  $t = 12$  hours. With the increase of the reaction time, a part of crystallites inside the microsphere are disappeared due to the combination action of Ostwald ripening and amphoteric phenomenon of ZnO.

Furthermore, the arrows in Panel b and c indicate the folded shell around the hole, which supports the mechanism that the holes are formed due to the expansion of the solvent inside the microspheres.

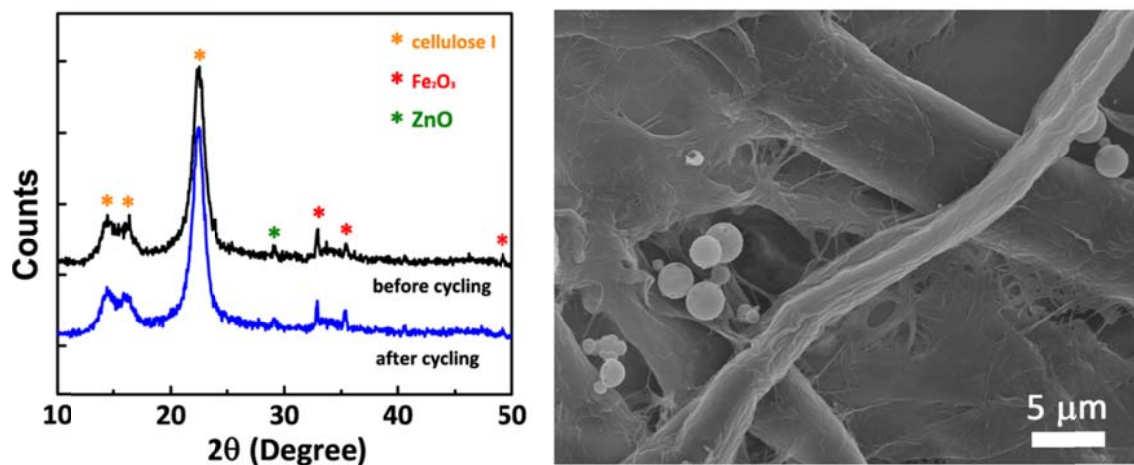


**Fig. S8** (a) XRD patterns for the photocatalytic paper before and after the recycling tests. (b) SEM image of the photocatalytic paper after the recycling test. The hollow spheres well maintain their structures.